Ionization in Hot Cavity Ion Sources

M. Turek*

Institute of Physics, Maria Curie-Skłodowska University, Pl. M. Curie-Skłodowskiej 1, 20-031 Lublin, Poland

*e-mail: mturek@kft.umcs.lublin.pl

A theoretical model of ionization and ion extraction in hot cavity ion sources is presented. The model enables the calculation of the total ionization efficiency in the hot cavity, as well as to study changes in the number of ions and neutral particles inside the cavity. A general formula describing the evolution of the system is derived — which could be especially useful for fast numerical calculations. Examples of calculation results are presented and discussed, showing that high ionization efficiencies (significantly exceeding the predictions of the Saha–Langmuir formula) can be achieved especially for small extraction openings. An alternative (to the ion and neutral numbers) description of the system has been proposed in terms of the total number of particles and the difference between the neutrals and the ions, which in some cases makes understanding the dynamics of the system much easier. The possibilities of the model are illustrated considering four special cases: closed cavity, cold cavity, and the cases of weak extraction and super-efficient extraction ("each ion" mode). The theoretical formulae enabling total ionization efficiency for the two latter cases are derived in the paper, and their predictions are compared to the results of numerical calculations.

topics: surface ionization, hot cavity ion sources

1. Introduction

The isotope on-line separation (ISOL) facilities employed a variety of different kinds of target–ion-source systems [1], including discharge, forced electron beam induced arc (FEBIAD), hollow cathode, electron cyclotron resonance (ECR) and other ion sources. Among them, the hot cavity thermal ionization ion sources are of significant importance. They were developed in the 1970s and employed mostly in nuclear spectroscopy to find new, usually unstable, isotopes [2, 3]. Ion sources of that kind were characterized by a simple construction and robustness. Moreover, they required the microamounts of the substance to be ionized in order to produce a high-quality ion beam with extreme purity and very low energy spread. This, combined with the fact that ions spent a very short time inside a cavity ionizer, made them ideal candidates for on-line separation of short-lived nuclides produced by bombardment of specially tailored targets by energetic beams [4–6].

In its "canonical" form, the most important part of the hot cavity is the semi-open, tubular ionizer (spherical ionizers have also been designed in [7, 8]). There are different approaches concerning the delivery of the substances to be ionized: (i) the ionizer could be connected to the irradiated target by linear transfer [7], (ii) the target is placed in contact with the ionizer [9], or (iii) the ionizer wall itself is an irradiated target releasing a variety of created nuclides directly into the hot ionizers cavity [10].

Large ionization efficiency of a hot cavity ion source is achieved due to the fact that the atoms to be ionized undergo numerous collisions (up to thousands) with the cavity walls, which leads to the ionization degrees of orders of magnitude larger than those predicted by the Saha–Langmuir equation, describing a single collision/surface ionization event. The general expression for ionization in thermal equilibrium is given by

$$\alpha = \frac{N_{ion}}{N_o} = G \exp\left(-\frac{V-\varphi}{k_{\rm B}T}\right), \tag{1}$$

where N_{ion} and N_o are respectively the numbers of ions and neutrals leaving the surface of temperature T. In (1), V and φ are the ionization potential of the atom and the work function of the ionizer, respectively, and G is a specific constant of the particle–surface combination, including e.g. reflection coefficients for ions and neutrals.

Despite the fact that the original construction was designed approximately fifty years ago, it still attracts the attention of scientists involved in nuclear spectroscopy, isotope separation and various ISOL projects [11, 12], as well as the precise determination of isotope ratio in geoscience studies [13–15].

It should be mentioned that hot cavity ion sources have evolved over the years into the resonant ionization laser ion sources (RILIS) [16–21]. Their principle of operation makes use of the stepwise excitation of the valence electron of atoms by high-power tunable lasers. In such solutions, a hot cavity

is used as a trap for atoms that undergo excitations and ionization by a high repetition rate laser beam. Due to the fact that the eigenstate energies are the fingerprint of each element and ion, the RILIS main feature is the extraordinary elemental selectivity.

Several attempts have been made to describe the processes taking place in hot cavity ion sources using computer modelling, especially those based on the Monte Carlo methods. Some of them focused on thermal ionization in the hot cavity [11, 22, 23], describing the crucial effect of multiple collisions with the walls of the hot cavity, while other papers presented issues such as vapour transport from the bombarded target to the ionizer [24, 25] or the release of nuclides from the walls of the ionizer [26, 27]. Various shapes of ionizers were considered in the literature; the most popular being tubular [23, 28–30], rarely employed spherical or hemispherical [31–33], but also conical [34–36], and even the most exotic, resembling a kind of mace with spikes [22]. Recently, a cavity having the shape of a flat disc was considered [37], being a case of tubular ionizer characterized by a very small length compared to its diameter, which results in a large number of particle–wall collisions during the particle's travel to the extraction aperture. Some versions of the numerical models were only suitable for stable (non-radioactive) nuclides, whilst the latter were upgraded to take into account the effects of radioactive decay and delays due to diffusion and effusion [32, 38]. It was also shown that in the case of hard-to-ionize nuclides, the other ionization mechanism included in the model, i.e., electron ionization, could also give a substantial contribution to the total ion source yield [28, 29, 32].

On the other hand, several theoretical models of ionization in the hot cavity have been proposed over the decades [39–43]. They are mainly based on the fact that a state of thermal equilibrium between the plasma and the particle-emitting hot walls is achieved. This results in a potential step that prevents positive ions from hitting the walls and losing their charge. In the other words — the plasma potential acts like an "ionization amplifier" [41]. However, there is an open question pointed out by the authors [40, 42] whether plasma in thermal equilibrium could be achieved in the condition of rather low gas pressure, typical for ion sources of this kind. A simple theoretical model was proposed based on a different approach, in which the evolution of the particles inside the ionizer was divided into a large number of stages engaging a single collision of each particle with the wall. The proposed model takes into account mostly the geometry of the ionizer [43]. Surprisingly, the variation of the model assuming the optimal extraction condition (each ion is extracted from the ionizer almost instantly after its creation) provides almost the same results as those discussed in [41, 42]. The model, which was proposed for stable nuclides, was later slightly improved to the case of radioactive species [38].

In the paper, a generalized version of the theoretical model discussed in [43] is presented. Some particular assumptions are made regarding the ionizer geometry, thus the model parameters take into account rather the probability of particle loss/extraction. As previously, the evolution of the system is discretized into stages, with the assumption that each particle hits the inner surface of the ionizer once during the stage. The changes in the numbers of ions and neutrals inside the cavity are calculated for the j-th stage and the general formula describing the evolution of the system is given — also in the matrix formalism, which could be especially useful for numerical calculations. Several general examples of results are presented and discussed. An alternative description of the system state has also been proposed in terms of the total number of particles and the difference between neutrals and ions, together with the formulae describing the evolution of the system. This new representation appears to be useful for the interpretation of system behaviour. Some special cases are also presented and discussed, including weak extraction, super-efficient extraction (so-called "each ion" mode [38, 43]), and also the cold cavity case. The proposed model can contribute to the understanding the processes taking place in various hot cavity ion sources.

2. The ionization model

Let us consider a cavity of the internal area S, with an extraction opening of the area S_e. A sketch of the ionizer cavity is shown in Fig. 1. One should keep in mind that the cavity does not have to be neither spherical nor characterized by any other symmetry. The only geometrical parameters of the model are the above-mentioned areas. The initial number of particles inside the cavity is denoted N_o. These particles can undergo ionization on the internal cavity surface and then leave it as ions. On the other hand, ions that are adsorbed on the surface could be neutralized. The probability of the ionization/neutralization, in other words, the ratio of the number of ions desorbing from the surface to the number of all particles leaving it (ions and neutrals), is defined by the Saha–Langmuir equation

$$\beta = \frac{N_{ion}}{N_o + N_{ion}} = \frac{a}{a+1}. \tag{2}$$

Some simplifications have been proposed in order to make the mathematical description easier. First of all, it is assumed that the process of ionization/extraction of all particles in the cavity is divided into an infinite number of short stages. Within one stage, each particle (neutral or ion) hits the surface once and undergoes ionization/neutralization with probability β. After that, the particles could leave the cavity with probability k^+ for ions and probability k for neutrals. The extraction probability for the neutral atoms can be estimated as
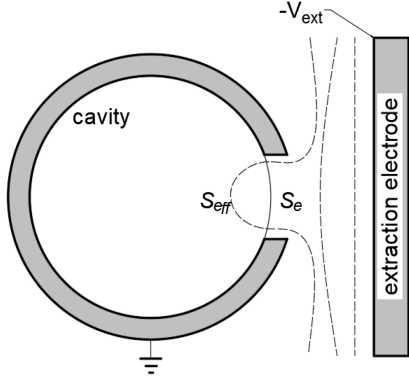
Fig. 1. Schematic view of the considered system. Note that the cavity does not have to be spherically symmetric.

the ratio of the area of the extraction opening S_e and the total area of the internal surface S. Thus,

$$k = \frac{S_e}{S}. \tag{3}$$

On the other hand, the probability k^+ for ions could reach a higher value, because the effective area S_{eff} of the extraction opening for ions is larger due to the penetration of the extraction field, as shown in Fig. 1, changing trajectories of charged particles.

Let us introduce the following annotations:

n_j — number of neutrals in the cavity at the j-th stage;

i_j — number of ions in the cavity at the j-th stage;

N_j' — number of neutrals leaving the cavity at the j-th stage;

I_j' — number of ions leaving the cavity (extracted) at the j-th stage;

N_j — number of neutrals left in the cavity at the j-th stage;

I_j — number of ions left in the cavity at the j-th stage.

In fact, there is a balance of the quantities

$$n_j = N_j + N_j',$$
$$i_j = I_j + I_j'. \tag{4}$$

As it was stated previously

$$N_j' = k\, n_j,$$
$$I_j' = k^+ i_j. \tag{5}$$

In the first stage, one has

$$i_1 = \beta N_o,$$
$$n_1 = (1 - \beta) N_o. \tag{6}$$

Similarly, one obtains the number of particles that stay in the cavity after the first stage, i.e.,

$$I_1 = \left(1 - k^+\right) i_1 = \left(1 - k^+\right) \beta N_o,$$
$$N_1 = (1 - k) n_1 = (1 - k)(1 - \beta) N_o. \tag{7}$$

Taking both ionization and neutralization into account, one obtains the numbers of particles in the second stage as

$$i_2 = \beta N_1 + (1 - \beta) I_1 =$$
$$\beta (1 - k) n_1 + (1 - \beta)\left(1 - k^+\right) i_1,$$

$$n_2 = (1 - \beta) N_1 + \beta I_1 =$$
$$(1 - \beta)(1 - k) n_1 + \beta\left(1 - k^+\right) i_1. \tag{8}$$

The general recursive relations for n_j and i_j are

$$i_{j+1} = (1 - \beta)\left(1 - k^+\right) i_j + \beta (1 - k) n_j$$
$$n_{j+1} = \beta\left(1 - k^+\right) i_j + (1 - \beta)(1 - k) n_j. \tag{9}$$

In turn, using the matrix formalism, the dynamics of the state of the system (described by $\boldsymbol{p}_j$ vector) could be written as

$$\boldsymbol{p}_{j+1} = A\,\boldsymbol{p}_j, \tag{10}$$

where

$$\boldsymbol{p}_j = \begin{pmatrix} i_j \\ n_j \end{pmatrix} \tag{11}$$

and

$$A = \begin{pmatrix} (1 - \beta)\left(1 - k^+\right) & \beta (1 - k) \\ \beta\left(1 - k^+\right) & (1 - \beta)(1 - k) \end{pmatrix}. \tag{12}$$

The total ionization efficiency of the ion source is the ratio of the number of ions extracted form the cavity to the number of all particles introduced into it (N_o). This can be written in the general form

$$\eta = \begin{pmatrix} \frac{k^+}{N_o} & 0 \end{pmatrix} \cdot \sum_{j=0}^{\infty} A^j \begin{pmatrix} i_1 \\ n_1 \end{pmatrix}. \tag{13}$$

The formula (13) could be very useful and easily applied to estimate the ionization efficiency using e.g. interactive tools like Matlab, Mathematica etc.

3. Results

Exemplary results of the calculations are presented in Fig. 2. The $\eta(\beta)$ curves were calculated for a relatively small size of the extraction opening $k = 0.01$ and three different values of k^+ (i.e., $2k$, $5k$, $10k$). One can see that all presented curves converge asymptotically for small β. On the other hand, for high ionization probabilities, a stronger extraction (or rather larger penetration of the extraction field) results in a higher total ionization efficiency, which is in a good agreement with the results obtained using numerical models [30–38]. The efficiency exceeds the predictions of the Saha–Langmuir formula and is higher than 0.5 even for $\beta = 0.01$, provided that k^+ is large enough.

Before the presentation of some chosen special cases, there should be introduced an alternative representation of the considered system, namely

$$P_j = n_j + i_j,$$
$$\Delta_j = n_j - i_j. \tag{14}$$
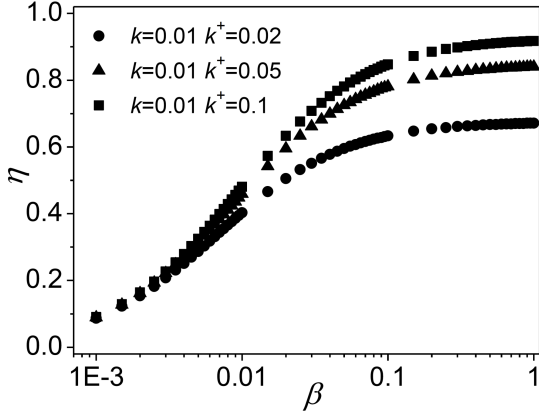
Fig. 2. Ionization efficiency as a function of β for different values of k and k^+ parameters.

The first quantity is just the total number of particles in the cavity (P_j), while the second quantity (Δ_j) is the difference between neutrals and ions and can have both positive and negative values. The inverse transformation could be easily obtained

$$n_j = \frac{P_i + \Delta_j}{2},$$
$$i_j = \frac{P_j - \Delta_j}{2}. \tag{15}$$

The dynamics of the system in (Δ, P) coordinates could be obtained from (8) and (15) after some tedious but straightforward calculations

$$P_{j+1} = P_j - \kappa^+ P_j + \kappa^- \Delta_j$$
$$\Delta_{j+1} = (1 - 2\beta)\left(\Delta_j + \kappa^- P_j - \kappa^+ \Delta_j\right), \tag{16}$$

where

$$\kappa^+ = \frac{k^+ + k}{2},$$
$$\kappa^- = \frac{k^+ - k}{2}. \tag{17}$$

The evolution of the system in both (n, i) and (Δ, P) coordinates is presented in Fig. 3a and b, respectively. The considered cases are the same as in Fig. 2.

The trajectories in the (n, i) coordinate set could be also approximated by two straight segments corresponding to the prevailing ionization and extraction phases. The curvature of the arc connecting these segments depends on the parameter k^+ — the stronger the extraction, the more rounded the trajectory and closer to the n axis (one has to keep in mind that i is the number of the ions inside the cavity, hence it gets smaller for larger k^+). One can also observe that the peak is shifted to higher n values as k^+ increases. In other words — maximal ionization is achieved sooner.

The shape of the trajectory in the (Δ, P) coordinates is a composition of two trends, i.e., the change of ionization degree (movement along the Δ
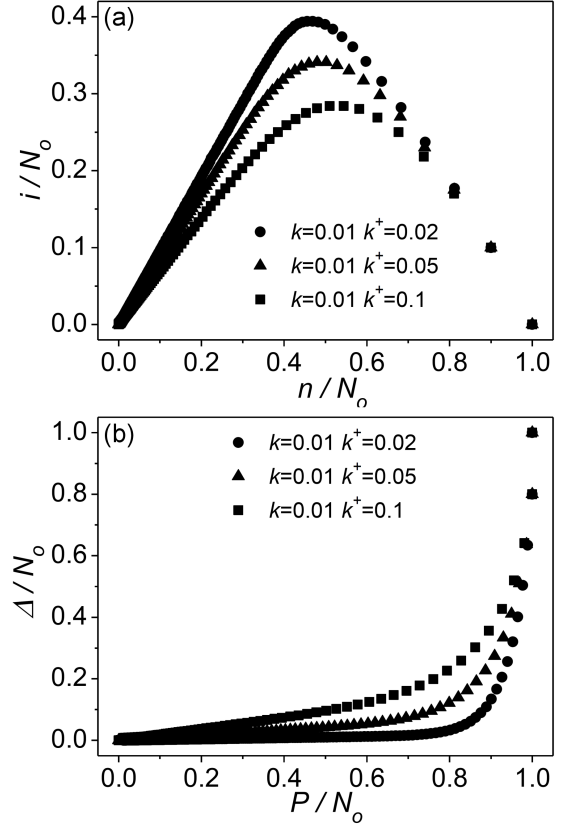
Fig. 3. Evolution of the system in (i, n) and (P, Δ) coordinates. The same cases are presented as in Fig. 2.
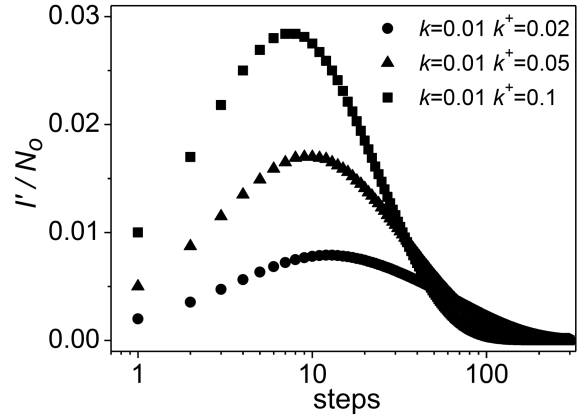
Fig. 4. Evolution of the number of extracted ions per stage/time unit.

axis) and the loss of particles, which is represented as the decrease of P. One can see that the trajectory starts at the (N_o, N_o) point and the first phenomenon dominates at the first phase of evolution, while the extraction prevails later on.

The evolution of the number of extracted ions for different values of k^+ is shown in Fig. 4. The stronger is the extraction (i.e., large k^+), the larger are the obtained I' values, which could be expected from the data in Fig. 3. Moreover, for larger k^+
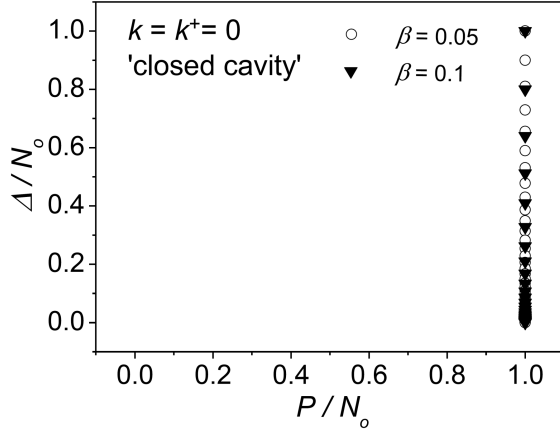
Fig. 5. Evolution of the system in the case of a closed cavity.

Fig. 6. Evolution of the system in the case of a cold cavity ($\beta = 0$, different values of k and k^+).

values, the maximum is achieved sooner, because the extraction can be considered to be more efficient: in the case of $k^+ = 0.1$, it is for $j = 7$, while for $k^+ = 0.02$ the much broader peak is observed for $j = 15$.

3.1. Special case — closed cavity

This case could be defined by putting $k = k^+ = 0$, i.e., no particle is able to leave the cavity. In that case, the A matrix has the form

$$A = \begin{pmatrix} (1-\beta) & \beta \\ \beta & (1-\beta) \end{pmatrix} \tag{18}$$

and (16) is simplified accordingly. It is quite straightforward to show that

$$P_{j+1} = P_j, \tag{19}$$

which means that particles are not lost due to the lack of extraction and

$$\Delta_{j+1} = (1-2\beta)\,\Delta_j, \tag{20}$$

which indicates that the amount of ions changes at a constant ratio in each step. Figure 5 presents the dynamics of the system in the (Δ, P) coordinates. One can see that the system moves along the line $P = N_o$ with a rate that depends largely on the ionization coefficient β. In this case, there is no point in considering the total ionization efficiency since no particles leave the cavity. However, it is easy to see that the amounts of ions and neutrals inside the cavity are equal when equilibrium is achieved ($\Delta = 0$).

3.2. Special case — cold cavity

In the considered case, ionization does not take place because the condition $\beta = 0$ is set. Having in mind that typical values of the ionization potential for a wide class of substances are several (or of the order of 10) eV, while the work function is usually smaller (say 4–5 eV), both α and β decrease with decreasing T, asymptotically approaching 0. The case $\beta = 0$ should be understood as a limiting

case when surface ionization is virtually impossible. The dynamics of the system is governed by the loss of particles with constant rates

$$i_{j+1} = \left(1-k^+\right)i_j \tag{21}$$

and

$$n_{j+1} = (1-k)\,n_j. \tag{22}$$

Dynamics in (Δ, P) coordinates is given by

$$P_{j+1} = P_j - \kappa^+ P_j + \kappa^- \Delta_j,$$
$$\Delta_{j+1} = \Delta_j + \kappa^- P_j - \kappa^+ \Delta_j. \tag{23}$$

As long as the condition $\Delta_o = P_o$ is true, one gets instantly

$$\Delta_j = P_j. \tag{24}$$

The evolution of the system in that regime is presented in Fig. 6. The system moves along the $\Delta = P$ line toward the $(0,0)$ point with a rate that increases with the probabilities k and k^+. As one can see, this rate increases twice as both k and k^+ are larger by a factor of 2. This is another limiting case as the area above the $\Delta = P$ line is inaccessible.

The total ionization efficiency could be calculated from (21) and (22) by summing up the extracted ions

$$\eta = \frac{k^+}{n_o + i_o} \sum_j i_j =$$
$$\frac{k^+}{n_o + i_o} i_o \left[1 + \left(1-k^+\right) + \left(1-k^+\right)^2 + \dots \right] =$$
$$\frac{i_o}{n_o + i_o} \tag{25}$$

The ionization efficiency in this trivial case is determined only by the initial number of ions in the cavity.

3.3. Special case — very small extraction voltage

Such a case could be described by the following condition $k^+ = k$. This means (according to formula (17)) that $\kappa^+ = k$ and $\kappa^- = 0$. This can be
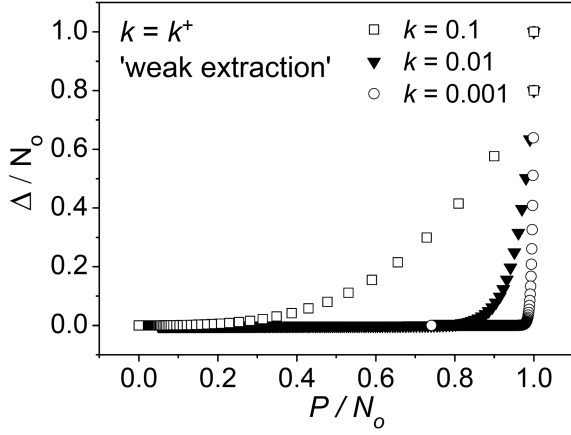
Fig. 7. Evolution of the system in the case of a weak extraction ($k = k^+$).
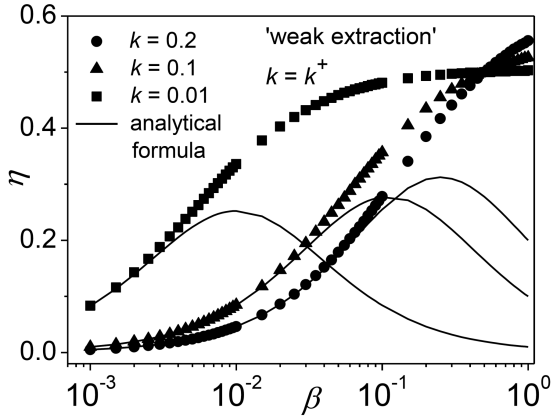
Fig. 8. Ionization efficiency as a function of β for different values of k in a case of weak extraction. The thin line represents the results predicted by the approximate formula (32).

achieved by applying a very small extraction voltage or in the case of a very small extraction opening. In such cases, the effective surface of the opening seen by the ion is the same as the geometrical surface of the opening. The transformation matrix (12) simplifies to

$$A = (1-k) \begin{pmatrix} (1-\beta) & \beta \\ \beta & (1-\beta) \end{pmatrix} \qquad (26)$$

The behaviour of the system can be expected to be similar to that of a "closed cavity" case, some distortion will be introduced by the factor $(1-k)$ leading to particle loss. Using an alternative coordinate set, one gets

$$P_{j+1} = (1-k)P_j,$$
$$\Delta_{j+1} = (1-k)(1-2\beta)\Delta_j. \qquad (27)$$

The evolution of the system is shown in Fig. 7. All calculations were done for $\beta = 0.1$. The shape of the trajectory depends on the k parameter. The smaller k is, the easier it is to see that the trajectory can be

approximated by two segments. The first of them lies on the line $P = N_o$, and the second one on the line $\Delta = 0$. A given course is achieved by the trajectory after approximately 10 steps. It should be mentioned that the trajectory becomes more and more rounded for larger extraction openings (larger k).

In the considered case, it is possible to derive an approximate formula that estimates the total ionization efficiency in the cavity for the cases of small β. Let us remind that after the first stage one has $i_1 = \beta N_o$ and $n_1 = (1-\beta)N_o$. Then, using transformation matrix (12), one can obtain

$$i_2 = 2\beta(1-\beta)(1-k)N_o$$

$$n_2 = \beta^2(1-k)N_o + (1-k)(1-\beta)^2 N_o \approx$$
$$(1-k)(1-\beta)^2 N_o. \qquad (28)$$

Note that the term containing β^2 has been omitted as very small. Repeating these calculations one obtains

$$i_3 = 3\beta(1-\beta)^2(1-k)^2 N_o,$$

$$n_3 = \beta^2(1-\beta)^2(1-k)^2 N_o$$
$$+ (1-k)^2(1-\beta)^3 N_o \approx (1-k)^2(1-\beta)^3 N_o. \qquad (29)$$

Generally,

$$i_j = j\beta(1-\beta)^{j-1}(1-k)^{j-1}N_o,$$
$$n_j \approx (1-k)^{j-1}(1-\beta)^j N_o. \qquad (30)$$

Keeping in mind that the total ionization efficiency is defined as

$$\eta = \frac{1}{N_o}\sum_j I_j', \qquad (31)$$

one obtains

$$\eta = \frac{k}{N_o}\sum_j j\beta(1-\beta)^{j-1}(1-k)^{j-1}N_o =$$
$$\frac{k\beta}{\left(1-(1-\beta)(1-k)\right)^2}, \qquad (32)$$

by using the formula

$$1 + 2x + 3x^2 + 4x^3 + \cdots = \frac{1}{(1-x)^2}. \qquad (33)$$

A comparison of the $\eta(\beta)$ curves obtained using (32) with the exact result using the general recipe (13) is shown in Fig. 8. One can see that the formula (32) perfectly fits the exact results for small values of β. The range of applicability of (32) increases fast with k — this formula provides good results up to $\beta = 0.003$ for $k = 0.01$, while for $k = 0.2$ it could be applied up to $\approx \beta = 0.07$. It should also be noted that the order of exact $\eta(\beta)$ dependences changes when β is larger than 0.6 (for substances that are easy to ionize) — in such case, higher efficiencies are achieved for a wider extraction opening.

3.4. Special case — each ion extracted

The "each ion" case is a hypothetical case where every ion is extracted from the cavity immediately after its creation. This could theoretically be achieved by a combination of a large enough extraction opening and a strong extraction field. Such a case was previously described in [43]. Each ion case can be described within the considered model by putting $k^+ = 1$ (and, hence, $\kappa^+ = k$ and $\kappa^- = 0$). The evolution of the system does not look much simplified in the (P, Δ) coordinates

$$P_{j+1} = P_j - \frac{1+k}{2} P_j + \frac{1-k}{2} \Delta_j,$$

$$\Delta_{j+1} = (1 - 2\beta) \left(\Delta_j + \frac{1-k}{2} P_j - \frac{1+k}{2} \Delta_j \right). \tag{34}$$

On the other hand, the behaviour of the system is very simple in the coordinates (n, i)

$$i_{j+1} = \beta (1 - k) n_j,$$

$$n_{j+1} = (1 - \beta) (1 - k) n_j, \tag{35}$$

and the number of ions produced in the j-th step depends only on the number of neutrals in the cavity.

The evolution of the system in the (P, Δ) space (shown in Fig. 9) looks surprisingly simple. The system moves along the straight lines in (P, Δ) coordinates as in the case of a cold cavity. However, its inclination depends on the ionization factor — the larger β is, the closer to the P axis ($\Delta = 0$ line) the trajectory lies. In the considered case, the rate of the evolution of the system increases with k.

Repeating the calculations similar to the previous case and keeping in mind (35) and (6), one obtains

$$i_2 = \beta (1 - \beta) (1 - k) N_o,$$

$$n_2 = (1 - \beta)^2 (1 - k) N_o,$$

$$i_3 = \beta (1 - \beta)^2 (1 - k)^2 N_o,$$

$$n_3 = (1 - \beta)^3 (1 - k)^2 N_o \tag{36}$$

and generally

$$i_j = \beta (1 - \beta)^{j-1} (1 - k)^{j-1} N_o,$$

$$n_j = (1 - \beta)^j (1 - k)^{j-1} N_o. \tag{37}$$

Hence, the ionization efficiency in the considered case can be calculated as

$$\eta = \frac{1}{N_o} \sum_j \beta (1-\beta)^{j-1} (1-k)^{j-1} N_o =$$

$$\frac{\beta}{1 - (1-\beta)(1-k)}, \tag{38}$$

using the formula for the sum of the geometrical series.

The formula (32) was also derived in [43] and has a large similarity to those presented in [41, 42].
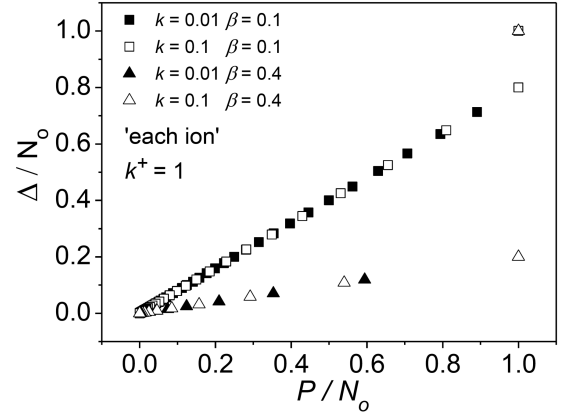
Fig. 9. Evolution of the system in "each ion" case ($k^+ = 1$).
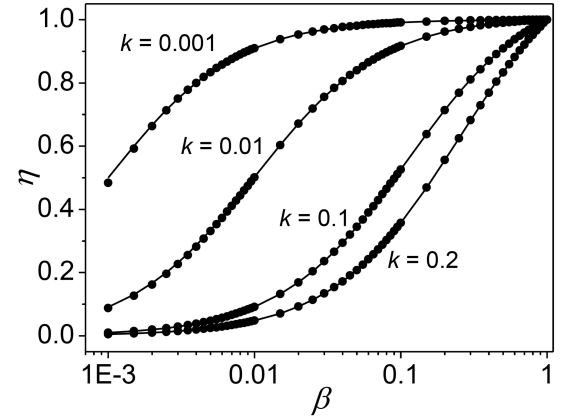
Fig. 10. Ionization efficiency as a function of β for different values of k in the "each ion" case. The thin line represents the results predicted by (38).

Figure 10 shows the ionization efficiency as a function of β for different k values. It could be seen that the smaller is the extraction opening, the larger the ionization efficiency is achieved even for very small values of the β parameter. This is, of course, due to the fact that each particle undergoes a larger number of collisions in such a case, and their chance to be ionized rises. It should be also noted that the predictions of formula (38), shown as the thin lines in Fig. 10, are in perfect agreement with the results of the general calculations according to (13). Importantly, one should keep in mind that (38) was derived without any simplifications.

4. Conclusions

A theoretical model of ionization in a hot cavity is presented. It is based on the discretisation of the evolution of the system and makes use of only a few parameters, involving the size of the extraction opening, the increase of the effective extraction opening size due to the extraction potential,

the area of internal ionizer surface etc. The model enables fast calculation of the evolution of the system as well as the total ionization efficiency. Some exemplary calculations show that the total efficiencies achieved in the hot cavity depend on the effective size of the extraction opening (which includes the effect of the extraction voltage) and reach the values exceeding by far the predictions of the Saha–Langmuir formula. Two different ways of describing the state of the system are considered in the paper. One of them is just the number of ions and neutrals in the cavity, the other one is the total number of particles and the difference between the neutral and ions numbers. Each of the two descriptions has its advantages and depending on the case can be more useful for the description of the evolution of the system. In the paper, four special cases/scenarios of ionization in a hot cavity are considered: closed cavity, cold cavity, case of weak extraction and an optimal "each ion scenario". For each of these cases, formulae describing the evolution are presented and different schemes of the system behaviour are discussed. Moreover, for the two latter cases, formulae enabling calculations of the total ionization efficiency are derived. Their predictions are compared to the results of numerical calculations. The presented model gives the opportunity of a better understanding of the dynamics of ionization processes taking place inside the hot cavity ion sources.

References

[1] R. Kirchner, *Nucl. Instrum. Methods Phys. Res. B* **204**, 179 (2003).

[2] G.J. Beyer, E. Herrmann, A. Piotrowski, V.I. Raiko, H. Tyroff, *Nucl. Instrum. Methods* **96**, 437 (1971).

[3] P.G. Johnson, A. Bolson, C.M. Henderson, *Nucl. Instrum. Methods* **83**, 106 (1973).

[4] V.A. Karnaukhov, D.D. Bogdanov, A.V. Demyanov, G.I. Koval, *Nucl. Instrum. Methods* **120**, 69 (1974).

[5] G.D. Alton, J.R. Beene, *J. Phys. G Nucl. Part. Phys.* **24**, 1347 (1998).

[6] E. Kugler, *Hyperfine Interact.* **129**, 23 (2000).

[7] G.D. Alton, Y. Liu, H. Zaim, S. N. Murray, *Nucl. Instrum. Methods Phys. Res. B* **211**, 425 (2003).

[8] P.A. Hausladen, D.C. Weisser, N.R. Lobanov, L.K. Fifield, H.J. Wallace, *Nucl. Instrum. Methods Phys. Res. B* **190**, 402 (2002).

[9] A. Osa, S.-I. Ichikawa, M. Matsuda, T.K. Sato, S.-C. Jeong, *Nucl. Instrum. Methods Phys. Res. B* **266**, 4394 (2008).

[10] V.G. Kalinnikov, K.Ya. Gromov, M. Janicki, Yu.V. Yushkevich, A.W. Potempa, V.G. Egorov, V.A. Bystrov, N.Yu. Kotovsky, S.V. Evtisov, *Nucl. Instrum. Methods Phys. Res. B* **70**, 62 (1992).

[11] P.V. Cuong, Ph.D. Thesis, Université Paris Sud, 2010.

[12] T.K. Sato, M. Asai, A. Borschevsky et al., *Nature* **520**, 209 (2015).

[13] J. R. Reimink, R. W. Carlson, T.D. Mock, *J. Anal. At. Spectrom.* **35**, 2337 (2020).

[14] A. Trinquier, C. Maden, A.-L. Fauré, A. Hubert, F. Pointurier, B. Bourdon, M. Schönbächler, *Anal. Chem.* **91**, 6190 (2019).

[15] C. Maden, A. Trinquier, A.-L. Fauré, A. Hubert, F. Pointurier, J. Rickli, B. Bourdon *Int. J. Mass Spectrom.* **434**, 70 (2018).

[16] Y. Liu, C.U. Jost, A.J. Mendez II et al., *Nucl. Instrum. Methods Phys. Res. B* **298**, 5 (2013).

[17] N. Lecesne, *Rev. Sci. Instrum.* **83**, 02A916 (2012).

[18] S.J. Park, J.B. Kim, *Hyperfine Interact.* **241**, 39 (2020).

[19] R. Li, M. Mostamand, J. Romans, *Hyperfine Interact.* **241**, 22 (2020).

[20] T. Day Goodacre, J. Billowes, K. Chrysalidis, D.V. Fedorov, V.N. Fedosseev, B.A. Marsh, P.L. Molkanov, R.E. Rossel, S. Rothe *Hyperfine Interact.* **238**, 41 (2017).

[21] K. Chrysalidis, A.E. Barzakh, R. Ahmed et al., *Nucl. Instrum. Methods Phys. Res. B* **463**, 472 (2020).

[22] C. Maden, H. Baur, A.-L. Fauré, A. Hubert, F. Pointurier, B. Bourdon, *Int. J. Mass Spectrom.* **405**, 39 (2016).

[23] M. Turek, K. Pyszniak, A. Drozdziel, J. Sielanko, *Vacuum* **82**, 1103 (2008).

[24] Y. Zhang, G.D. Alton, *Nucl. Instrum. Methods Phys. Res. B* **241**, 947 (2005).

[25] Y. Zhang, G.D. Alton, *J. Vac. Sci. Technol. A* **23**, 1558 (2005).

[26] B. Mustapha, J.A. Nolen, *Nucl. Instrum. Methods Phys. Res. B* **204**, 286 (2003).

[27] B. Mustapha, J.A. Nolen, *Nucl. Instrum. Methods Phys. Res. A* **521**, 59 (2004).

[28] M. Turek, K. Pyszniak, A. Droździel, *Vacuum* **83**, S260 (2009).

[29] M. Turek, *Acta Phys. Pol. A* **123**, 847 (2013).

[30] M. Turek, A. Drozdziel, K. Pyszniak, D. Maczka, B. Slowinski, *Rev. Sci. Instrum.* **83**, 023303 (2012).

[31] M. Turek, *Acta Phys. Pol. A* **120**, 188 (2011).

[32] M.Turek, *Acta Phys. Pol. A* **128**, 935 (2015).

[33] M. Turek, *Acta Phys. Pol. A* **128**, 931 (2015).

[34] M. Turek, *Acta Phys. Pol. A* **132**, 259 (2017).

[35] M. Turek, *Przegląd Elektrotechniczny* **94**, 66 (2018).

[36] M. Turek, *Acta Phys. Pol. A* **136**, 329 (2019).

[37] M. Turek, *Devices Methods Meas.* **11**, 132 (2020).

[38] M. Turek, *Vacuum* **104**, 1 (2014).

[39] A. Latuszynski, V.I. Raiko, *Nucl. Instrum. Methods* **125**, 61 (1975).

[40] V.P. Afanas'ev, V.A. Obukhov, V.I. Raiko, *Nucl. Instrum. Methods* **145**, 533 (1977).

[41] R. Kirchner, *Nucl. Instrum. Methods Phys. Res. A* **292**, 203 (1990).

[42] M. Huyse, *Nucl. Instrum. Methods* **215**, 1 (1983).

[43] A. Latuszyński, K. Pyszniak, A. Droździel, M. Turek, D. Mączka J. Meldizon, *Vacuum* **81**, 1150 (2007).